*Journal of the European Ceramic Society* **15** (1995) 405–413
Elsevier Science Limited
Printed in Great Britain.
0955-2219/95/$9.50

# Vickers and Knoop Indentation Behaviour of Cubic and Partially Stabilized Zirconia Crystals

G. A. Gogotsi, S. N. Dub, E. E. Lomonova & B. I. Ozersky

Institute for Problems of Strength of the Academy of Sciences of Ukraine, Timiryazevskaya str. 2, Kiev 252014, Ukraine

(Received 30 December 1993; revised version received 27 June 1994; accepted 22 September 1994)

***Abstract***

*Hardness and fracture toughness of cubic zirconia crystals (CZC) doped with yttria and partially stabilized zirconia crystals (PSZC) doped with yttria, terbia and ceria were studied at indentation loads of 0·1–300 N. MOR and* $K_{Ic}$ *of these materials were measured under bending conditions. A maximum hardness value of* $H_K$ *= 21·2 GPa was obtained for CZC at a 0·1 N indentation load when a longer diagonal of the Knoop indenter being directed along <110>. Starting from a 2 N load, PSZC exhibited lateral cracks and phase transition zones. Radial cracks in Vickers indentation tests of Y–Tb–PSZC and Y–Ce–PSZC appeared above 40 N and 50 N respectively. Such cracks in Knoop indentation tests were observed above 300 N. Orientation anisotropy of lateral cracks was noticed in all crystals, radial ones were revealed only in CZC. After grinding off the specimen surfaces, lateral cracks were found to be present under the impressions. The calculations of fracture toughness* $K_{Ic}^{v}$ *using the equation proposed by the authors gave a value corresponding to those materials determined on bending.*

## 1 Introduction

The fact that zirconia single crystals can be used for medical[1,2] and other cutting instruments stimulates studies on their surface fracture toughness (Fig. 1). The results obtained also appear useful[3] for understanding mechanical behaviour of the materials of such a group. In investigations, both Vickers[4,7] and Knoop indenters[5,8,9] were used. Cubic (CZC), i.e. completely stabilized[5,6,10,11] and partially stabilized crystals (PSZC)[4,9,14] doped with yttria (Y–PSZC) attracted specific interest. The crystals doped with calcia,[4] magnesia,[1,4,8] terbia[9,12] and ytterbia,[2,14] i.e. containing additives with an ionic radius smaller or larger than that of zirconia were also studied. PSZC of lower fracture toughness were tested at indentation loads which did not usually exceed 10 N[3,15] and crystals of higher fracture toughness were investigated at the same loads[1,4,11,16] that are usually for advanced ceramics. The indentation was performed on the (001),[3,5,11] (011)[3,8] or on arbitrarily oriented planes.[2,9,14,17] The comparison of data[2,11] shows no essential differences in $K_{Ic}$ values for Y–PSZC obtained on different indentation planes. The equations used[11,18] give critical stress intensity factors $K_{Ic}^{v}$ obtained in indentation tests which agree with $K_{Ic}$ values determined in SENB bending. Such coincidences were not usually observed in the rest of the cases.

The Vickers indentation caused considerable anisotropy of hardness and fracture toughness for CZC[11] and certain anisotropy of fracture toughness for PSZC.[3] At room temperature, Y–PSZC exhibited[16] considerable influence of the Vickers indenter orientation on phase transition processes on the (001) plane. Similar crystals[15] also revealed phase transition zones around such impression above 200°C. It was found that at room temperature it occured only within the plastic zone of impression. The Knoop indenter caused considerable anisotropy both of hardness and of fracture processes for Y–CZC[5] and Y–PSZC.[2,8]

Y–CZC are the most extensively studied materials. The indentation behaviour of Y–PSZ (though being more interesting for structural applications) is not clear enough and there is no information available which is necessary for their positive practical application. It should be noted that all the data published on PSZC can be divided into two groups: those which was mainly obtained for stronger crystals of Ceros Corp.[3,6,15] and those obtained for tougher crystals produced in the former USSR.[1,2,9,14] The investigations of the first group pursued physical goals, the studies on the latter were aimed at the elucidation of possible practical fields of application of such crystals. In the present work we used a wider range of loads and focused our major attention on PSZC.

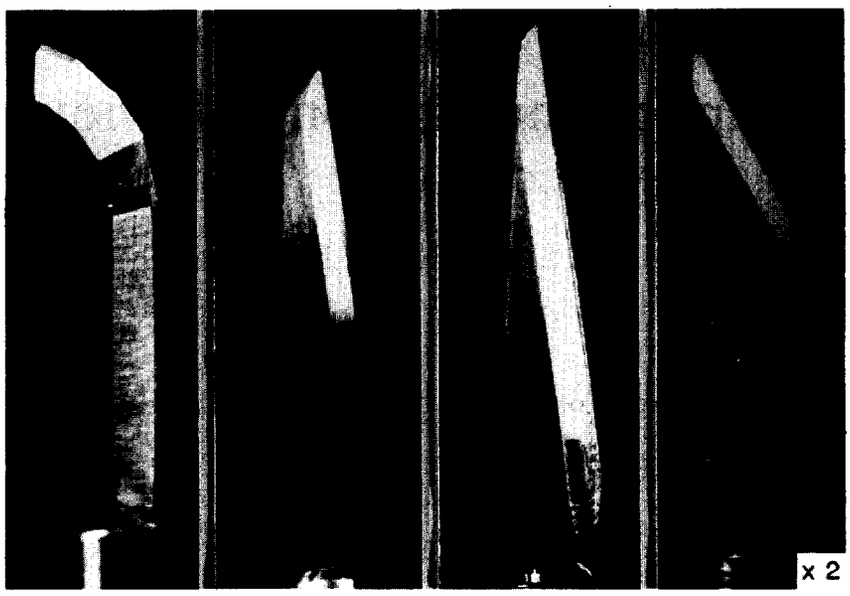


**Fig. 1.** Experimental samples of surgical knives with blade sharpening radii equal to 0·2–0·5 μm, made of the zirconia crystals studied. They were tested in clinics of Kiev, Moscow and Sydney (×2).

## 2 Materials and Methods

The crystals under study were grown by a skull melting technique[19] from zirconia powders of a purity over 99·9% (the purity of other components was higher than 99·99%). A K-1 material (Y–CZC) (Table 1) contained 10 mol% $Y_2O_3$,[20] a K-2 material[12] contained 3·3 mol% $Y_2O_3$ and less than 0·3 mol% terbia and in a K-3 material[21] ceria was added instead of terbia. After pounding the pieces of specimens in a corundum mortar, they were investigated by X-ray phase analysis. It was established that the K-1 powder consisted of a 100% zirconia cubic phase, the K-2 powder contained 30% monoclinic and 70% tetragonal phases, the K-3 material was 50% monoclinic and 50% tetragonal and cubic.

Test specimens (3·5 × 5 × 45 $mm^3$ bars) were cut, ground and polished with a diamond instrument. The orientation of specimens was determined by Laue back-reflection which revealed that all their surfaces coincided with the (001) planes. Thus, on mechanical tests, a fracture crack propagated in the (001) plane and tensile stresses and impression also appeared in the same plane.

MOR on four-point bending, static moduli of elasticity and critical stress intensity factors $K_{1c}$ were determined by procedures[22] evaluated earlier in numerous tests of different advanced ceramics and single crystals. For $K_{1c}$ measurements, the specimens were notched for a half-thickness depth and placed with their 3 mm wide surface on supports with a 20 mm span between loading rollers (for MOR measurements the loading surface was 5 mm wide).

The Knoop indentation tests at 0·1–10 N loads were performed in an MXT-70 microhardness meter (Matsuzawa, Japan). For 50–300 N loads a Ceramtest device of our production was used. The hardness was calculated by $H_k = 14{\cdot}23\ P/o^2$, where $P$ is the load on the indenter and $d$ is the length of a larger diagonal of the Knoop impression.

The $H/E$ relationship determined according to the concepts of Ref. 23 was calculated by the equation:

$$H/E = \frac{0{\cdot}14 - b/d}{0{\cdot}45}$$

where $b$ is the length of a shorter diagonal of the Knoop indenter.

The Vickers indentation at 0·1–10 N loads was tested in the same microhardness meter. For high loads, (50–300 N), a TP-2 Vickers hardness meter and Ceramtest device were used.

The values of $H_V$ were calculated by

$$H_v = 0{\cdot}4636\ P/a^2$$

where $a$ is the Vickers impression diagonal half-length.

To calculate critical stress intensity factors $K_{1c}^V$ the following equations were used

$$K_{1c} = 0{\cdot}016\ (E/H)^{0{\cdot}5} P/C^{1{\cdot}5} \quad (1)^{24}$$

$$K_{1c} = 0{\cdot}018\ H\ a^{0{\cdot}5}\ (E/H)^{0{\cdot}4}/C/a - 1)^{0{\cdot}5} \quad (2)^{11}$$

**Table 1.** Average mechanical characteristics of crystals on fracture in the <001> direction

| *Material* | *Static modulus of elasticity* | *MOR, MPa* | *$K_{1c}$, Pa $m^{1/2}$ (on bending)* |
|---|---|---|---|
| K-1 | 327 | 224 | 2·01 (1·41)[a] |
| K-2 | 350 | — | 9·96 |
| K-3 | 369 | 1250 | 11·43 |

[a]Obtained on the specimen with a sharp crack.

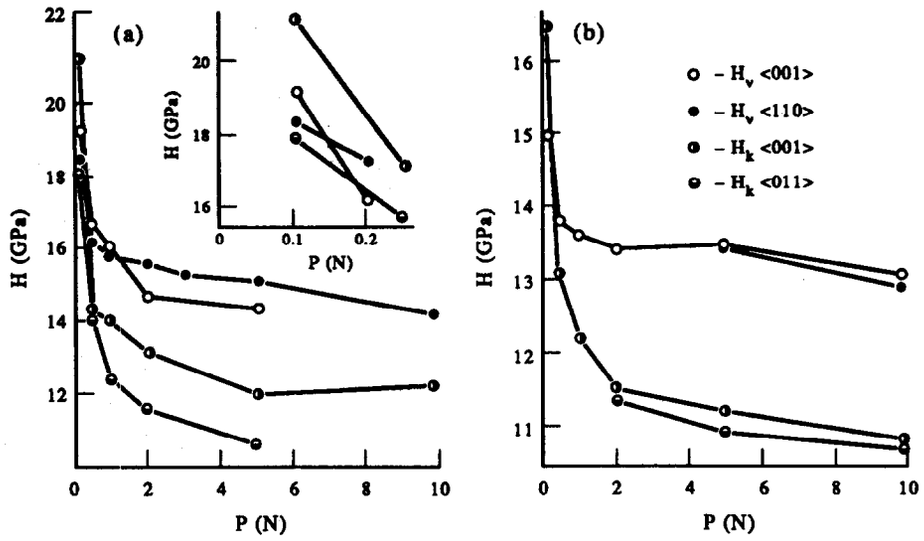


**Fig. 2.** Microhardness $H$ of K-1 crystals (a) and K-3 crystals (b) as a function of indentation load and indenter orientation (crystallographic directions of the Vickers indenter diagonal (index V) and larger diagonal of the Knoop indenter (index K).

**Table 2.** Hardness (GPa) at a 4·9 N load

| *Material* | *Interdenter diagonal direction* | |
|---|---|---|
| | *<001>* | *<011>* |
| K-1 | 14·4 / 12·0 | 15·1 / 10·7 |
| K-2 | 13·6 / 11·4 | 13·6 / 11·1 |
| K-3 | 13·6 / 11·2 | 13·6 / 10·9 |

The left hand value is the Vickers hardness, the right hand value is the Knoop hardness.

$$K_c^v = 0{\cdot}0424\ (PE/a)^{0{\cdot}5}/(C/a)^{1{\cdot}57} \qquad (3)^{25}$$

Indented specimen surfaces were studied using an NU-2E optical microscope (Carl Zeiss Jena, Germany).

## 3 Results

Microhardness values for K-1 cubic and K-3 partially stabilized crystals, as a function of applied loads at the orientation of indenter diagonals in the <001> and <110> directions, on the (001) plane for the loads up to 10 N, are shown in Fig. 2. (For K-2 crystals the picture was about the same.) It should be noted that partially stabilized crystals (as opposed to cubic ones) do not practically exhibit any anisotropy of microhardness on the (001) plane for both indenters (Table 2). Vickers impressions on K-1 crystals in the <001> direction of indenter diagonals were almost completely fractured at loads above 5 N; in the <001> direction this fracture occurred at loads above 10 N. (For the Knoop indenter the picture was quite the opposite.)

In Vickers indentation tests, lateral cracks appeared with the indenter diagonals in the <001> direction (Fig. 3(a)) and zones (probably pressure-induced phase transformation[16] of tetragonal phase to monoclinic symmetry) arose if they were in the <110> direction (Fig. 3(b)). In Knoop indentation tests, similar phase transition zones were revealed microscopically in phase contrast with

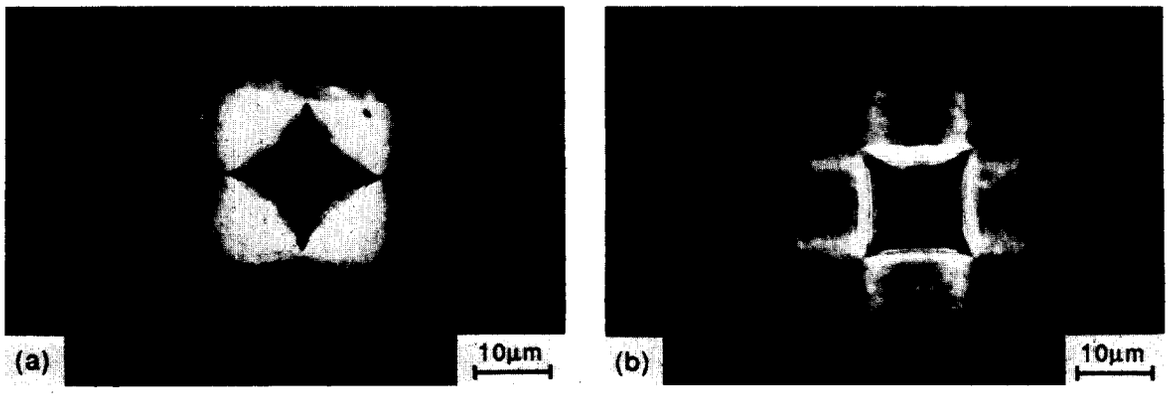


**Fig. 3.** Vickers impressions on the (001) plane of a K-3 crystal at a 10 N load: the diagonal coincides with the <100> direction (a) and with the <110> direction (b). Illumination: phase contrast.

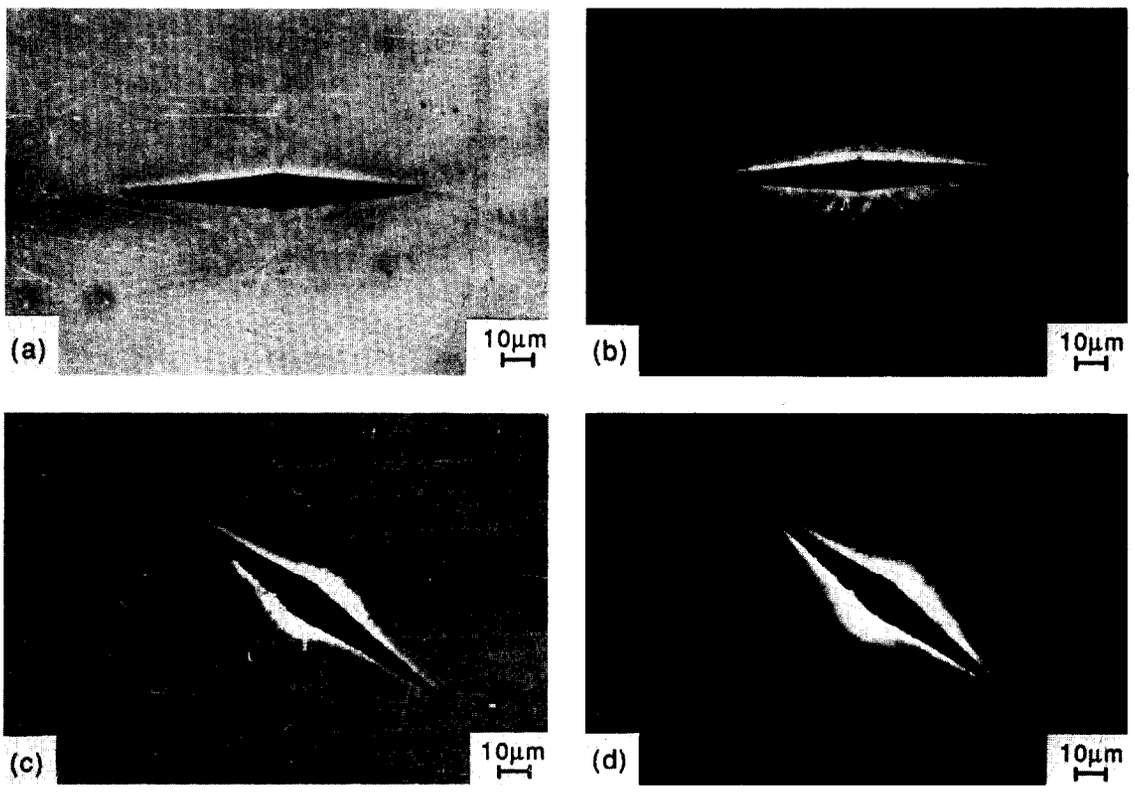


**Fig. 4.** Knoop impressions on the (001) plane at a 10 N load with a larger diagonal coincides with <001> (a,b) and with <110> (c,d). Illumination: reflected light (a,c), phase contrast (b,c).

the <001> direction of a larger diagonal (Fig. 4(a,b)). When this diagonal was in the <110> direction (Fig. 4(c)), lateral cracks appeared around the impression (more details in Ref. 26).

The results of studying the effect of elastic recovery of Knoop impressions are summarized in Table 3. They demonstrate that the influence of crystal anisotropy on $H/E$ values appeared to be quite noticeable for all the cases.

For the crystals under study, the relationship (up to 10 N loads) between the Vickers impression diagonal half-length and indentation loads is described by the equations:

$$a = 5{\cdot}4\ P^{0{\cdot}52} \quad \text{for K-1}$$
$$a = 5{\cdot}83\ P^{0{\cdot}51} \quad \text{for K-2}$$
$$f = 5{\cdot}81\ P^{0{\cdot}51} \quad \text{for K-3}$$

The Knoop indenter diagonal lengths are described by the equations:

$$d = 31{\cdot}12\ P^{0{\cdot}56} \quad \text{for K-1}$$
$$d = 33{\cdot}22\ P^{0{\cdot}54} \quad \text{for K-2}$$
$$d = 33{\cdot}46\ P^{0{\cdot}55} \quad \text{for K-3}$$

Only PSZC were investigated at higher indentation loads. The results of diagonal and crack measurements and $H_V$ and $K_{1c}$ calculations on the (001) plane, with the <001> direction of indenter

**Table 3.** Results of investigation of the relation $H/E$

| *Material* | *Load, N* | *Direction of the larger diagonal of the Knoop indenter* | | | | | | | | | |
|---|---|---|---|---|---|---|---|---|---|---|---|
| | | *<001>* | | | | | *<011>* | | | | |
| | | *d* | *b* | *d/b* | $H_K$ | *H/E* | *d* | *b* | *d/b* | $H_K$ | *H/E* |
| K-1 | 1 | 31·6 | 3·5 | 9·03 | 14·0 | 14·1 | 33·6 | 3·7 | 9·08 | 12·4 | 14·6 |
| | 2 | 46·0 | 5·0 | 9·20 | 13·2 | 14·0 | 49·0 | 5·7 | 8·97 | 11·6 | 18·2 |
| | 5 | 76·2 | 8·3 | 9·18 | 12·0 | 14·0 | 80·9 | 9·4 | 8·61 | 10·7 | 18·1 |
| | 10 | 108·6 | 12·1 | 8·96 | 11·8 | 15·2 | — | — | — | — | — |
| K-2 | 1 | 33·8 | 3·1 | 10·90 | 12·2 | 9·1 | — | — | — | — | — |
| | 2 | 49·0 | 5·0 | 9·80 | 11·6 | 11·6 | 49·5 | 5·9 | 8·39 | 11·4 | 20·6 |
| | 5 | 78·1 | 8·2 | 9·53 | 11·4 | 12·5 | 79·2 | 9·6 | 8·25 | 11·1 | 22·7 |
| | 10 | 111·7 | 11·8 | 9·47 | 11·2 | 12·7 | 113·6 | 13·9 | 8·17 | 10·8 | 24·2 |
| K-3 | 1 | 33·8 | 3·5 | 9·66 | 12·2 | 12·0 | — | — | — | — | — |
| | 2 | 49·2 | 5·0 | 9·84 | 11·5 | 11·5 | 49·4 | 6·0 | 8·23 | 11·4 | 23·3 |
| | 5 | 79·0 | 8·6 | 9·19 | 11·2 | 14·0 | 80·0 | 10·0 | 8·00 | 10·9 | 28·3 |
| | 10 | 113·9 | 13·0 | 8·76 | 10·8 | 16·8 | 114·3 | 14·4 | 7·93 | 10·7 | 30·0 |

**Table 4.** Results of hardness and fracture toughness tests on the (001) plane

| *Material* | *Load, N* | *Half-diagonal length a, μm* | *Crack length c, μm* | *Vickers hardness, GPa* | *Critical stress intensity factor $K^v_{Ic}$, MPa m calculated by* | | |
|---|---|---|---|---|---|---|---|
| | | | | | *1* | *2* | *3* |
| | 49·1 | 43·1 | 77·5 | 12·2 | 6·3 | 6·3 | 10·9 |
| | 98·1 | 61·1 | 126·4 | 12·2 | 6·0 | 6·5 | 10·4 |
| | 147·2 | 76·1 | 170·8 | 11·8 | 5·9 | 6·6 | 10·0 |
| K-2 | 196·2 | 86·6 | 202·8 | 12·1 | 6·0 | 6·8 | 10·1 |
| | 245·3 | 97·0 | 232·0 | 12·1 | 6·1 | 7·1 | 10·4 |
| | 294·3 | 107·4 | 265·9 | 11·8 | 6·0 | 7·2 | 10·2 |
| | 49·1 | 43·3 | 67·1 | 12·1 | 7·8 | 7·6 | 13·7 |
| | 98·1 | 61·5 | 112·6 | 12·0 | 7·2 | 7·3 | 12·5 |
| | 147·2 | 75·7 | 124·2 | 11·9 | 9·4 | 9·2 | 16·4 |
| K-3 | 196·2 | 86·3 | 180·6 | 12·2 | 7·1 | 7·6 | 12·1 |
| | 245·3 | 96·4 | 209·1 | 12·2 | 7·1 | 7·8 | 12·1 |
| | 294·3 | 106·6 | 249·9 | 12·0 | 6·6 | 7·5 | 11·2 |

diagonals are summarized in Table 4. These data complement our information published earlier (Table 5). The discrepancy between our data and those of other authors observed in this Table may be connected with some distinctions between the technologies of the growth of crystals and raw materials for them.

The radial cracks around Vickers impressions usually aligned with their diagonals, however, in several cases the picture was similar to that shown in Fig. 5.

The cracks around the Knoop impression were mainly lateral up to 300 N loads (Fig. 6). Only single radial cracks were noticed around some of them. The same picture existed in the tests of


**Fig. 5.** Vickers impression on the (001) plane of a K-3 crystal at a 200 N load (diagonals coincide with the <110> direction). Illumination: phase contrast.

**Table 5.** Hardness data reported in the literature

| *Hardness, GPa* | | *Load, N* | *Indentor orientation* | | $Y_2O_3$ *contains mol.%* | *Authors* |
|---|---|---|---|---|---|---|
| Vickers | *Knoop* | | *Plain* | *Direction* | | |
| *Y-CZC* | | | | | | |
| 16·1 | — | 5 | — | — | 20·0 | Ingel *et al.*[4] |
| — | 14·4 | 5 | (100) | <100> | | Hannink & Swain[8] |
| — | 12·1 | 5 | (100) | <110> | 14,3 | |
| 15·2 | — | | (100) | <100> | | |
| 15·2 | — | | | <110> | | Pajares *et al.*[5] |
| — | 14·0 | 2 | (100) | <100> | 9·4 | |
| — | 12·4 | 2 | | <110> | | |
| 15·6 | — | | (100) | — | | |
| 15·0 | — | 2-3 | (111) | — | 9·5 | Morscher *et al.*[6] |
| 14·5 | — | | (110) | — | | |
| 15·6 | — | 2 | (100) | <110> | 10·0 | Dub & Gogotsi[11] |
| Y-PSZC | | | | | | |
| 13·6 | — | 5 | — | — | 5 | Ingel *et al.*[4] |
| 15·0 | — | 1 | (100) | <100> | 3·5 | Martinez-Fernandez *et al.*[3] |
| 15·0 | — | 5 | (100) | <110> | 3·4 | Martinez-Fernandez *et al.*[15] |
| 12·0 | — | 50 | | | 2·3 | Saiki *et al.*[16] |
| 13·9 | — | 100 | — | — | 3+0·3%$T_2O_3$ | |
| 13·4 | — | 100 | — | — | 1·5+1·5% $Yb_2O_3$ | Gogotsi *et al.*[9] |
| 13·1 | — | 100 | — | — | 3·0 | |
| 12·8-13·8 | — | 10 | — | — | — | Gogotsi *et al.*[12] |
| 12·2-13·0 | — | 100 | — | — | 3+0·3% $Tb_2O_3$ | |
| 13·2 | — | 100 | — | — | 3 | Gogotsi & Swain[17] |
| 13·5 | — | 2 | (100) | <110> | 3 | |
| 12·1 | — | 49·1 | (100) | <110> | 3 | Dub & Gogotsi[11] |

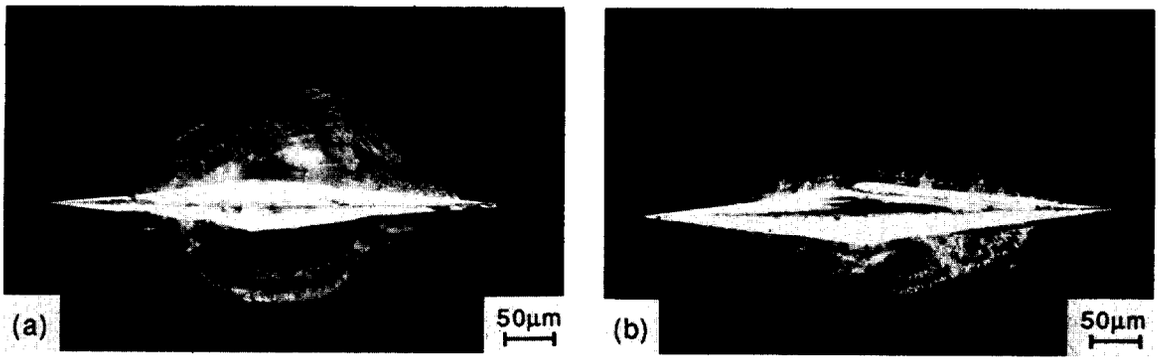


**Fig. 6.** Knoop impression on the (001) plane of a K-3 crystal at a 200 N load with a larger diagonal coincides with <001> (a) and with <110> (b). Illumination: polarized light.

crystals in Refs 2 and 9, when only at 400 N were pairs of radial cracks observed.

## 4 Discussion

### 4.1 Microhardness and hardness

From the analysis of data in Fig. 2, one can see that the maximum values of $H_V$ and $H_K$ we presented for K-1 cubic crystals are higher than those published[16] for the material of the same composition, but it is associated with the fact that in the present work, lower loads were used for indentation. At the same time in Ref. 5, for the <001> direction on (001), the authors obtained $H_V$ = 17·6 GPa and $H_K$ = 19 GPa at 0·5 N, while we obtained 16·5 GPa and 14·3 GPa, respectively. It should be noted that with higher loads this difference becomes less noticable (see Table 5). A descending curve of microhardness versus load is also characteristic of partially stabilized crystals, especially up to 10 N loads. At high loads, as follows from Table 4, it is practically a straight line. The values of $H_V$ for other yttria-stabilized crystals also appear to be quite close.[9] It is interesting that for K-2 crystals the dependence is also about the same, with $H_V$ measurements without strict crystallographic orientation of indentation planes (Table 5). These data point to the fact that $H_V$ values without indication of the load at which they were obtained, should be taken into account with great care.

If the above information on the values of $H_V$ and $H_K$ does not contradict the data published earlier, the relationships for $(E/H)^{1/2}$ given in Table 3 are somewhat different from the results of earlier investigations of cubic crystals, e.g. Ref. 5, where the relationship between these values and the Knoop indenter orientation were not elucidated. As it should be expected, the hardness of crystals is dependent on the orientation of the Knoop indenter (Figs 2 and 6) and they are also characterized by the anisotropy of elastic moduli.[27] Thus the value of $H/E$ determined from the Knoop impression is also orientationally dependent. It should be noted that, e.g. for K-1 crystals, d/D = 8·61 and $H/E$ = 18·1 were obtained in the <001> indentation direction at 5 N loads and in Ref. 5 these values for the same load were 8·3 and 22·0 N respectively. Such differences can be connected with certain differences in the production technology of the crystals under study.

However we could not succeed in getting values of elastic moduli in Knoop indentation tests comparable with those presented in Table 1. There is an impression that the approach[21] to the determination of elasticity (or $H/E$) of crystals requires a better understanding.

### 4.2 Fracture

Since the present fracture studies of cubic crystals did not reveal any new results compared to those found earlier[11] and published by other authors, we considered it expedient to discuss and revise only the results for partially stabilized crystals. Single radial cracks in these crystals started appearing around the corners of the Vickers impression at the following loads:

When the Vickers indenter diagonal was parallel to <110>, single radial cracks were observed at 40 N in a K-2 material and at 50 N in a K-3 material.

**Table 6**

| *Material* | *Indenter diagonal parallel to* | |
|---|---|---|
| | *<100>* | *<110>* |
| K-2 | 50 | 70 |
| K-3 | 40 | 50 |

(Lateral cracks in the <100> direction were discussed earlier.) The difference in sizes on the turn of indenter on the (001) plane at a 100 N indentation load, can be seen in Fig. 7 (the picture was more

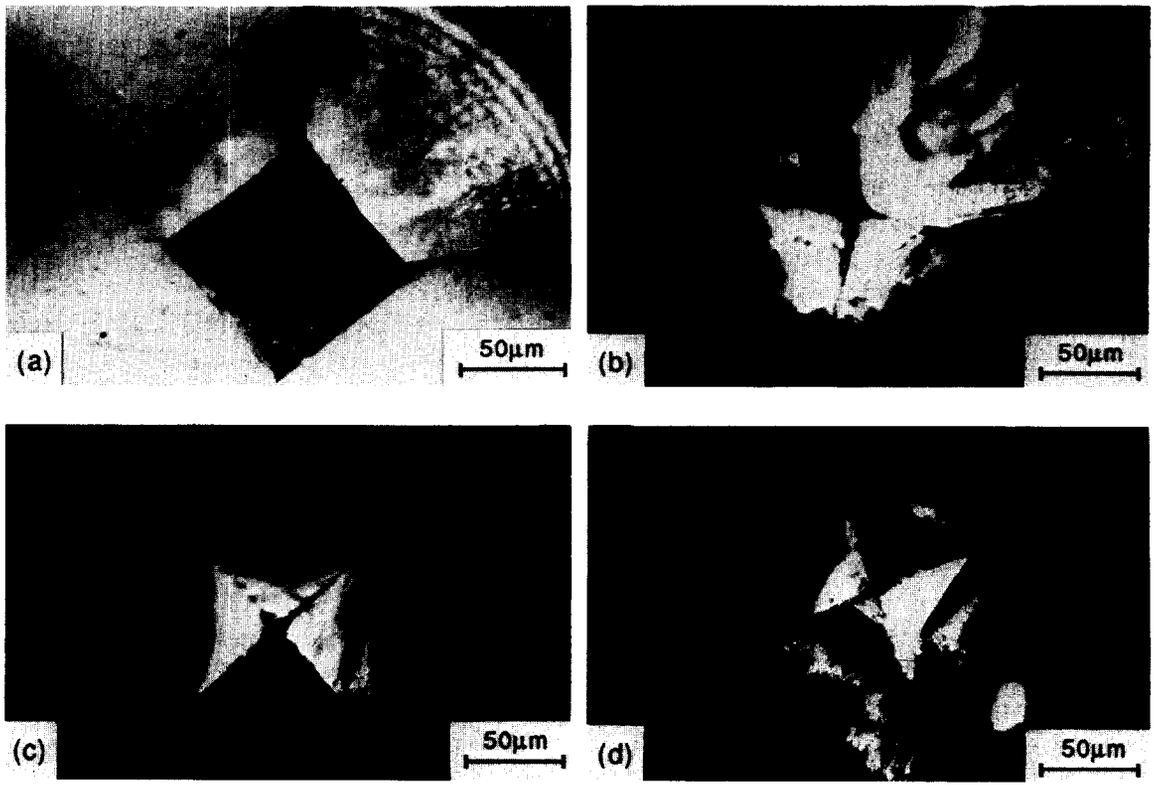


**Fig. 7.** Vickers impression on the (001) plane of a K-3 crystal at a 100 N load. Diagonals of the indenter correspond to the <100> direction (a,b), to the <110> direction (c) and are deflected through 30° from the <100> direction (d). Illumination: reflected light (a) and polarized light (c,d,e).

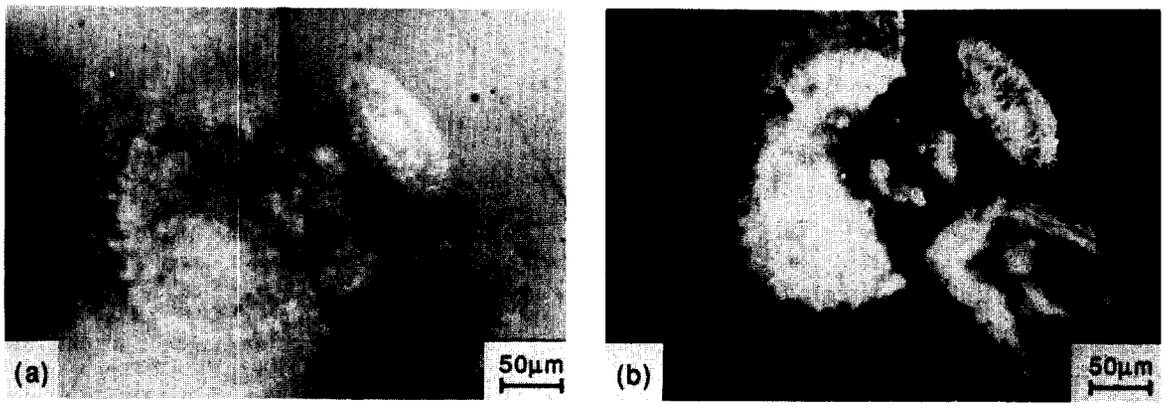


**Fig. 8.** Vickers impression on the (001) plane of a K-2 crystal after grinding off of its surface at a 100 N load. Illumination: reflected light (a) and polarized light (b).

or less identical for both materials). When the specimen surface is ground off in the indentation zone, lateral cracks can not only reach the surface, but also appear below the indenter impression, as is seen in Fig. 8. It should be noted that in Ref. 2 only lateral cracks reaching the surface are shown in Fig. 10. The lateral cracks in those crystals similar to those shown in Fig. 8 were not analyzed. Radial cracks usually propagating as Palmqvist cracks within the range of loads under study seemed to be branched in the subsurface layer (Fig. 9). Thus, their extent (fractured area) appeared larger than that which could be measured by optical microscope, since only one crack was revealed on the specimen surfaces under study.

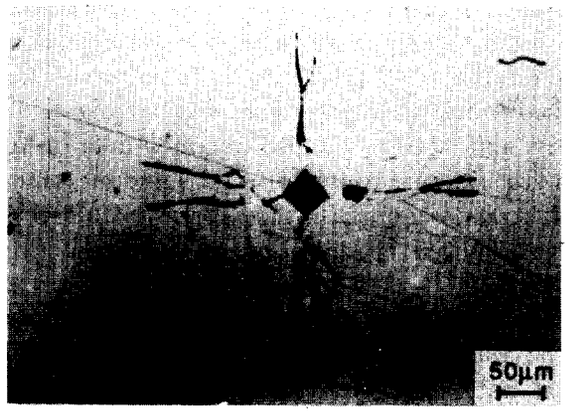


**Fig. 9.** Vickers impression on the (001) plane at a 200 N load with the diagonal coincides with <001> after partial grinding off of the surface. Illumination: reflected light.

This examination demonstrates that for a well-grounded judgment of the crystal capacity to resist local damages, one should take into account all the real features of their fracture on indentation.[2]

The estimates of their fracture toughness was based only on the measurement of the extent of radial cracks on the surface visible in reflected light in an optical microscope, which is usually done by investigators, (Table 4) and can probably be considered only as a first approach. However, if we take into account that any publications devoted to detailed investigations of PSZC fracture are practically non-existent, the data of the present work can be compared with the known ones only within the framework of this first approach. From Table 4 we can see that the values of $K_{1c}^{v}$ calculated by the equation[11] are quite close to the values of $K_{1c}$ measured on bar bending, (Table 1). If we compare the calculation results for $K_{1c}^{v}$[25] obtained in the case of arbitrary orientation of the indenter[2] on SC=3b surfaces with the results for Y–PSZC[11] obtained on the (100) plane with the <110> diagonal direction, (Table 4), one can see that they are very close. So we can assume that if elastic moduli of crystals are similar, the anisotropy of local fracture toughness is probably insignificant for practical purposes. The above crystals as well as the crystals in Ref. 11 exhibit higher fracture toughness than those presented, e.g. in Ref. 3 and investigated in an unannealed state. At the same time they display longer (by 20–40%) radial cracks originating on Vickers indentation than those revealed, e.g. in Ref. 9 during the studies on partially stabilised and tetragonal polycrystalline zirconia ceramics[17] doped with 3 mol.% yttria.

## 5 Conclusion

The investigations of cubic and partially stabilized zirconia crystals resulted in data on their hardness and fracture toughness variations during indentation on the (001) plane as a function of loads applied to the indenters, their diagonal aligned with <001> and <110>. We also obtained data on their strength, fracture toughness and static modulus of elasticity on bending (in this work we studied partially stabilized crystals doped with terbia, ceria and yttria).

It is shown that the equation proposed earlier by the authors for estimating $K_{1c}^{v}$ from the indentation data can give values very close to those determined for $K_{1c}$ in bending tests which cannot be achieved using other similar equations. For example it was noticed that at a 2 N load the Vickers indenter diagonals aligned with <001> lateral crack are formed and when the diagonals are aligned with <110>, phase transition zones appear. When a larger diagonal of the Knoop indenter is aligned with <001>, phase transition zones are also formed. At comparatively high (over 50 N) loads, partially stabilized crystals do not display any noticeable anisotropy of hardness or fracture toughness.

A lower fracture toughness of crystals doped with terbia as compared to those doped with ceria reveals not only lower values of $K_{1c}^{v}$ of the former, but also as lower loads giving rise to lateral cracks in the latter. In both crystals, lateral cracks appeared under the Vickers impression. We consider that the evaluation of fracture toughness on indentation of crystals should account for all their fracture features but not only for the length of radial cracks as it is usually done.

## Acknowledgements

This study was supported by the State Committee for Science and Technology of Ukraine. The authors are also grateful to the International Science Foundation of Soros for financial support of this work.

## References

1. Gogotsi, G. A., Mechanical behaviour of a new structural material: partially-stabilized $ZrO_2$ crystals. Informal seminar strength, reliability and quality assurance of components of engineering ceramics, Freiburg. 2–9 July 1992, IPP, Kiev, P. 24.
2. Gogotsi, G. A., Lomonova, E. E. & Pejchev V. G., Strength and fracture toughness of zirconia crystals. *J. Eur. Ceram. Soc.*, **11** (1993) 123–32.
3. Martinez-Fernandez, J., Jimenez-Melendo, M., Dominguez-Rodriguez, A., & Heuer, A., Elevated temperature studies of microindentation of Y–PSZ. In *Structural Ceramics–Processing Microstructural and Properties*, ed, J. J. Bentzen *et al.* Riso National Laboratory, Roskline, Denmarc, (1990) 413–8.
4. Ingel, R., Lewis, R. P. D., Bender, B. A. & Rice, R. W., Physical, microstructural, and thermomechanical properties of $ZrO_2$ single crystals. In *Science and Technology of Zirconia II. Advanced in ceramics*, **12** (1984) 408–13.
5. Pajares, A., Guiberteau, F., Dominguez-Rodriguez, A. & Heuer, A. H., Microhardness and fracture toughness anisotropy in cubic zirconium oxide crystals. *J. Amer. Ceram. Soc.*, **7** (1988) 332–3.
6. Morscher, G., Pirouz, P. & Heuer, A. H., Temperature dependence of hardness in yttria-stabilized zirconia single crystals. *J. Amer. Ceram. Soc.*, **3** (1991) 491–500.
7. Pajares, A., Guiberteau, F., Dominguez-Rodriguez, A., & Heuer, A. H., Indentation-induced cracks and the toughness anisotropy of 9·4-mol.% yttria-stabilized cubic zirconia single crystals. *J. Amer. Ceram. Soc.*, **4** (1991) 859–62.
8. Hannink, R. H. J. & Swain, M. V., Induced Plastic Deformation of Zirconia. In *Deformation of ceramic materials II*, ed, R. F. Tressler & R. C. Bradt. Plenum Press, N. Y. (1984) 695–708.

9. Gogotsi, G. A., Ozersky, B. A. & Oksametnaya, O. B., Behaviour of poly-and monocrystalline zirconia on indentation. *Refractory*, **33** (1992) 453–461.
10. Cook, R. F. & Pharr, G. M., Direct observation and analysis of indentation cracking in glasses and ceramics. *J. Amer. Ceram. Soc.*, **4** (1990) 787–817.
11. Dub., S. N. & Gogotsi, G. A., Indentation fracture toughness of zirconia crystals. *Materials Forum* (in press).
12. Gogotsi, G. A., Galenko, V. I., Ozersky, B. A., Lomonova, E. E., Myzina, V. A. & Kalabukchova, V. E., Strength and fracture toughness of yttria and terbia-doped zirconia crystals. *Refractory*, **34** (1993) 303–12.
13. Michel, D., Mazerolles, L., Perez, Y & Jorba, M., Fracture of metastable tetragonal zirconia crystals. *J. Mat. Sci.*, **18** (1983) 2618–28.
14. Gogotsi, G. A., Drosdov, A. V. & Pejchev, V. G., Mechanical behaviour of zirconia crystals partially stabilized with yttria. *Strength of Materials*, **23** (1991) 86–91.
15. Martinez-Fernandez, J., Jimenez-Melendo, M., Dominquez-Rodriguez, A. & Heuer, A. J., Microindentation-induced transformation in 3·5 mol.% yttria–partially–stabilized zirconia single crystals. *J. Amer. Ceram. Soc.*, **5** (1991) 1071–81.
16. Saiki, A., Ishizawa, N., Misutani, N. & Kato, M., SEM observation of the stress-induced transformation by Vickers indentation in Y–PSZ crystals. *J. Ceram. Soc. Jpn. Inter. Ed.*, **97** (1989) 41–6.
17. Gogotsi, G. A. & M. Swain, M. V., Comparison of strength and fracture toughness of single and polycrystalline zirconia. In *Science and Technology of Zirconia, V*, ed S. P. S. Badeval, M. J. Bannister & R. H. J. Hannink. Technomic Pub. Co, Lancaster-Basel (1993) 347–59.
18. Liang, K. M., Orange, G. & Fantozzi, G., Evaluation by indentation of fracture toughness of ceramic materials. *J. Mat. Sci.*, **25** (1990) 202–14.
19. Gogotsi, G. A., Lomonova, E. E. & Osiko, V. V., Studies mechanical characteristics of zirconia single crystals for structural application. *Refractory*, **32** (1991).
20. Gogotsi, G. A., Lomonova, E. E. & Ostrovoy, D. Yu., Deformation of $ZrO_2$ single crystals. *Refractory*, **33** (1992) 152–8.
21. Gogotsi, G. A. & Lomonova, E. E. (in preparation for publication).
22. Gogotsi, G. A., Test method of advanced ceramics: reasonable approaches for standardisation ceramics. *Key Engineering Materials*, **56–7** (1991) 419–34.
23. Marshall, D. B., Noma, T. & Evans, A. G., A simple method for determining elastic modulus to hardness ratios using Knoop indentation measurements. *J. Amer. Ceram. Soc.*, **65** (1992) 175–6.
24. Antis, G. R., Chanticul, B. R., Lawn, B. R. & Marshall, D. B., A critical evaluation of indentation techniques for measuring fracture toughness. *J. Amer. Ceram. Soc.*, **69** (1981) 533–8.
25. Niihara, K., A fracture mechanics analysis of indentation-induced Palmquist crack in ceramics. *J. Mat. Sci. Let.*, **2** (1983) 221–3.
26. Dub, S. N., Gogotsi, G. A. & Lomonova, E. E., Hardness and fracture toughness of $ZrO_2$ crystals with yttria and terbia (in preparation for publication in *J. Mat. Sci. Let.*).
27. Ingel, R. & Lewis, R. P. D., Elastic anizotropy in zirconia single crystals. *J. Am. Cer. Soc.*, **71** (1988) 265–71.